Alaa Elbinawi, Mogahed Al-abyad*, Karima E. Abd-Elmageed, Khaled F. Hassan, and Ferenc Ditroi

Proton induced nuclear reactions on natural antimony up to 17 MeV

DOI 10.1515/ract-2015-2483
Received July 18, 2015; accepted November 8, 2015; published online December 14, 2015

Abstract: The activation cross sections of proton induced reactions on ^{nat}Sb target leading to the formation of the radioisotopes ^{121m,g,123m}Te were measured. The experimental excitation functions were compared with the theoretical model calculations using the codes EMPIRE-3.1 and TALYS-1.4. The integral yields of the three radionuclides were calculated and the possibility of their production is discussed.

Keywords: Excitation function, stacked-foil technique, ^{nat}Sb targets, nuclear model calculations, yield.

1 Introduction

Nuclear reaction cross sections have various practical applications in science and technology. Charged-particle accelerators and nuclear reactors are commonly employed to produce radionuclides of interest. The physical basis of radionuclide production is optimized by using nuclear cross section data. Therefore, among the various types of nuclear data, the cross sections have great significance in the production and quality control of the desired radionuclides [1, 2]. Proton-induced reaction cross sections on natural antimony are important for various practical applications such as medical radionuclide production, thin layer activation (TLA) analysis, dosimetry application, etc. [3].

Antimony is an important element in several technical applications. Some of the radioisotopes produced on antimony have potential for use in several areas. This work deals with the production of some of those radionuclides.

The interaction of antimony with light ions has not been studied extensively [4, 5]. The aim of this study was to provide additional well established experimental cross-section data on proton induced reactions on natural antimony and thus to improve the quality of the data available in the literature.

2 Nuclear model calculations

With a view to validating the data and testing the predictive power of the nuclear theory, reaction cross sections were calculated theoretically using the nuclear model codes EMPIRE-3.1 [6, 7] and TALYS-1.4 [8]. Only the default parameters were used.

3 Experimental

3.1 Irradiations

High-purity antimony (99.999%) of natural isotopic composition (^{121}Sb: 57.21%; ^{123}Sb: 42.79%), supplied by Sigma-Aldrich, Germany and high-purity Al and Cu foils (99.999%, supplied by Goodfellow, England) were used to prepare thin targets by sedimentation onto 25 μm thick aluminium backings [9–11] and 10 μm thick aluminium wrapping. Copper foils were used to monitor the beam current. Two sets of targets were used. Each set consisted of 5 Sb foils and 3 Cu monitor foils. Targets were irradiated in a stacked-foil arrangement [12] which is not only economical but also assures a good relative accuracy. Each irradiation was for one hour with a proton beam of primary incident energy 17 MeV of constant current about 150 nA at MGC-20E cyclotron of the Institute for Nuclear Research, Hungarian Academy of Sciences, Debrecen, Hungary (ATOMKI). The degradation of energy within the stack was calculated using the SRIM code [13].

A monitor foil was placed in front of each stack, at which the beam energy is well defined, to accurately measure the beam flux. The energy of the extracted beam was

***Corresponding author: Mogahed Al-abyad,** Physics Department, Cyclotron Facility, Nuclear Research Centre, Atomic Energy Authority, Cairo 13759, Egypt, e-mail: alabyad_m@yahoo.com
Alaa Elbinawi, Khaled F. Hassan: Physics Department, Cyclotron Facility, Nuclear Research Centre, Atomic Energy Authority, Cairo 13759, Egypt
Karima E. Abd-Elmageed: Department of Physics, Faculty of Science, Benha University, Egypt
Ferenc Ditroi: Institute for Nuclear Research (ATOMKI), H-4026, Hungarian Academy of Sciences, Debrecen, Hungary

derived from the accelerator setting. The stacks were irradiated with a well-collimated beam in a target holder, which served also as a Faraday cup to collect the charge of the incident particles and evaluate the particle flux. The beam parameters were adapted by evaluating the excitation functions of the monitor reaction $^{nat}Cu(p,x)^{65}Zn$. Cross-section data for the monitor reaction were taken from the recommended data base of IAEA [14]. A good agreement between our values and recommended values was observed.

The energy and intensity of the beam from the cyclotron were checked using nuclear reactions $^{63}Cu(p,2n)^{62}Zn$, $^{63}Cu(p,n)^{63}Zn$ and $^{65}Cu(p,n)^{65}Zn$. The energy was determined from the curves of $[\sigma_{(62Zn)}/\sigma_{(63Zn)}]$ and $[\sigma_{(62Zn)}/\sigma_{(65Zn)}]$ ratios as a function of proton energy [15, 16].

3.2 Measurement of radioactivity

After appropriate cooling time the radioactivity measurement was started. The irradiated samples and monitor foils were measured using a high resolution gamma ray spectrometer consisting of HpGe "Canberra" detector coupled with a multichannel analyzer. The detector efficiency was determined experimentally using a selected set of gamma ray standard sources. The resulting spectra were analyzed using the software Maestro, version 5.0, supplied by EG&G ORTEC.

3.3 Calculation of total and isomeric cross sections

Using the well-known formula for the formation of an activation product, the cross section σ corresponding to a certain thin foil in the stacked target was calculated.

$$\sigma = MZe\lambda C/\left[xfN_A I_\gamma Q e^{-\lambda T_1}\left(1 - e^{-\lambda T_2}\right)\left(1 - e^{-\lambda T_3}\right)\right] \quad (1)$$

where: C is the measured photopeak area; λ is the decay constant (1/s); M is molar weight of the target; Q is the total collected charge during the irradiation; Ze is the projectile charge; x is the target thickness (g/cm^2); f is the isotopic abundance of the target isotope involved in the reaction; I_γ is the intensity of the measured gamma photon; N_A is Avogadro's number; T_1, T_2 and T_3 are the cooling, measuring and irradiation times.

When two isotopes or isomers have a common or very close γ-lines, with the knowledge of cross section of one of them and the area under peak of the common line, we can deduce the other cross section of the isotope or the isomer as follows:

Let there be two isomeric states (g and m) for an isotope with the supposed photopeak areas C_g and C_m respectively, and the common contributed photo peak C:

$$C = C_g + C_m \quad (2)$$

If we calculate the cross section of the ground state σ_g^* (using Equation 1) at the common γ-line considering as this line released only from ground state.

Then

$$\sigma_g^* = \sigma_g + \sigma_g \frac{C_m}{C_g} \quad (3)$$

With the same steps we have:

$$\sigma_m^* = \sigma_m + \sigma_m \frac{C_g}{C_m} \quad (4)$$

From Equations (3) and (4)

$$\sigma_g^* = \sigma_g + \sigma_g \frac{\sigma_m}{\sigma_m^* - \sigma_m} \quad (5)$$

Rearranging Equation (5)

$$\sigma_m = (1 - \frac{\sigma_g}{\sigma_g^*})\sigma_m^* \quad (6)$$

So the unknown cross section of the isomeric state σ_m can be calculated from a knowledge of the ground state cross section and the cross section calculated using the unseparated line ($\sigma_g^* + \sigma_m^*$).

The decay data used in the calculations are given in Table 1. They were taken from Refs. [17, 18].

3.4 Estimation of uncertainties

The uncertainties in the cross sections were estimated by using the error propagation through the formula used for calculation [19]. The contributions from non-linear parameters was ignored (time, half-life). The total uncertainty was estimated by taking the square root of the sum of all individual contributions into quadrature, detector efficiency (7%), the peak area fit (3%), the foil thickness (3%), The time error including irradiation, cooling and measuring (1%), the beam flux (7%), incident particle intensity (5%). The total uncertainty in the cross section values was about 12%.

Table 1: Decay data of Te isotopes produced in the present study.[a]

Nuclide	Half-life ($T_{1/2}$)	Decay mode (%)	E_γ (keV)	I_γ (%)	Contributing reactions	Threshold energy[b] (MeV)
^{121g}Te	19.17 d	EC (100)	573.1	80.4	^{121}Sb$(p,n)^{121g}$Te	1.85
					^{123}Sb$(p,3n)^{121g}$Te	17.74
^{121m}Te	164.2 d	IT (88.6)	212.2	81.5	^{121}Sb$(p,n)^{121m}$Te	2.14
		EC (11)			^{123}Sb$(p,3n)^{121m}$Te	18.04
		β^+ (0.001)				
^{123m}Te	119.2 d	IT (100)	159.0	84	^{123}Sb$(p,n)^{123m}$Te	1.09

[a] Taken from Ref. [17, 18];
[b] Calculated as given in Ref. [20].

4 Results and discussion

4.1 Cross sections

The experimental reaction cross sections and their uncertainties are given in Table 2. The data are plotted as a function of proton energy in Figures 1, 2 and 3 in comparison with the results of nuclear model calculations as well as literature experimental data [21].

4.1.1 ^{nat}Sb$(p,xn)^{121g}$Te reaction

^{121}Te has two isomeric states, the ground state ^{121g}Te ($T_{1/2}$ = 19.17 d) and a metastable state ^{121m}Te ($T_{1/2}$ = 164.2 d). The ^{121g}Te decays by 100% EC mode to ^{121}Sb while emitting a few gamma lines. The radionuclide ^{121g}Te can be produced in the ^{121}Sb(p,n) and ^{123}Sb$(p,3n)$ reactions. The activity of ^{121g}Te was assessed through measurement of the E_γ = 573 keV gamma line. ^{121g}Te is produced directly in the proton bombardment and also indirectly by decay of the isomer ^{121m}Te (IT = 88.6%). The half-life of ^{121m}Te ($T_{1/2}$ = 164.2 d) is longer than that of the ground state ^{121g}Te, therefore cross section measurement of the direct production of this isomeric state is not possible without separation of the contributing processes. Using Equation (6) and subtracting the contribution of ^{nat}Sb$(p,x)^{121m}$Te from the measured total peak area, the cross section of the ^{nat}Sb$(p,x)^{121g}$Te direct process could be determined. Doing this separation the overall uncertainty of the measured cross section points of the

Table 2: Cross sections for the formation of some radionuclides in proton induced nuclear reactions on ^{nat}Sb.

Energy[a] (MeV)	Cross section (mb)		
	^{121g}Te	^{121m}Te	^{123m}Te
16.8 ± 1.1	19.8 ± 2.2	19.6 ± 2.2	12.8 ± 1.4
16.0 ± 1.2	28.4 ± 3.3	30.9 ± 3.6	18.5 ± 2.1
14.4 ± 1.3	48.3 ± 5.8	42.8 ± 5.1	25.6 ± 3.1
14.4 ± 1.3	67.9 ± 8.5	59.8 ± 7.5	28.3 ± 3.5
12.8 ± 1.5	75.8 ± 9.9	45.2 ± 5.9	52.0 ± 6.8
11.4 ± 1.6	101.5 ± 13.7	88.3 ± 11.9	52.2 ± 7.0
9.1 ± 1.8	141.2 ± 19.8	84.7 ± 11.9	87.1 ± 12.2
7.3 ± 2.0	80.5 ± 11.7	30.0 ± 4.4	39.0 ± 5.7
6.0 ± 2.0	28.5 ± 4.3	26.2 ± 3.9	14.8 ± 2.2
4.3 ± 2.1	5.7 ± 0.9	5.3 ± 0.8	7.0 ± 1.1

[a] The deviation describes the energy spread within the target sample.

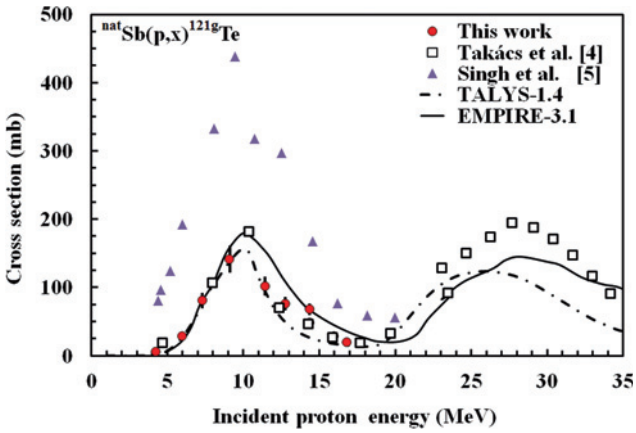

Fig. 1: Excitation function of the ^{nat}Sb$(p,x)^{121g}$Te reaction.

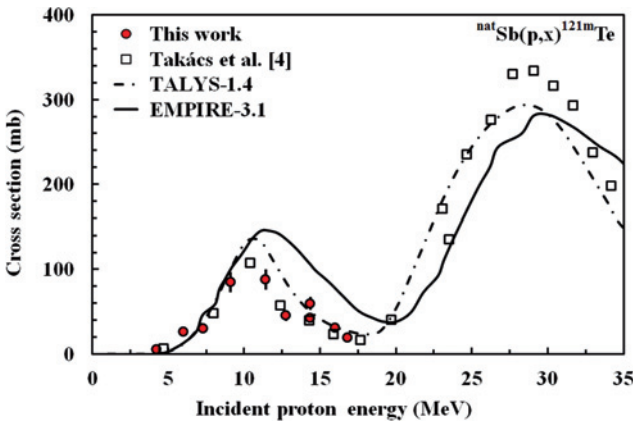

Fig. 2: Excitation function of the ^{nat}Sb$(p,x)^{121m}$Te reaction.

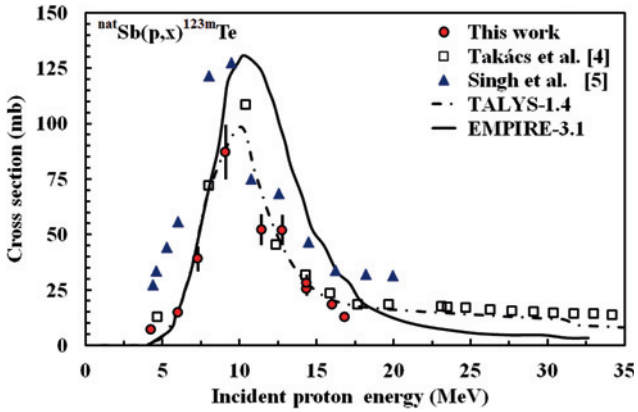

Fig. 3: Excitation function of the $^{nat}Sb(p, xn)^{123m}Te$ reaction.

$^{nat}Sb(p, x)^{121g}Te$ reaction increased due to the uncertainty in cross section calculations of ^{121m}Te.

The experimental data are presented in Figure 1 together with the results of codes calculations and the available literature data [4, 5]. The excitation function has two maxima, the first at about 10.6 MeV and the second at about 28 MeV. In the present work only the $^{121}Sb(p, n)$ reaction contributes to the measured data. Above 17.7 MeV the $^{123}Sb(p, 3n)$ reaction starts contributing to the excitation function. The present experimental data are in good agreement with Takács et al. [4], while Singh et al. [5] have the same trend but with higher values of the cross section because they did not separate the contribution of ^{121m}Te. The data obtained by the TALYS-1.4 code are in good agreement with the experimental data; also the EMPIRE-3.1 code gives acceptable agreement but with slightly higher values.

4.1.2 $^{nat}Sb(p, xn)^{121m}Te$ reaction

The ^{121m}Te ($T_{1/2}$ = 164.2 d) decays to the ground state by isomeric transition (IT = 88.6%) and to ^{121}Sb by EC+β^+ (11.4%). The decay is followed only by one relatively intense gamma line (E_γ = 212.2 keV, I_γ = 81.5%) and several weak lines. The activity of ^{121m}Te was assessed via the most intense 212.2 keV γ-line. The present experimental data as well as the results of the theoretical codes are presented in Figure 2. The excitation function of this reaction has also two peaks; the former due to the $^{121}Sb(p, n)$ reaction and the latter is formed due to $^{123}Sb(p, 3n)$. In the present work the maximum cross-section value of 100 mb at about 10.5 MeV renders the contribution of the (p, n) reaction only, due to the limited energy.

Only one data set is available in the literature [4], and there is an acceptable agreement between it and the present work. The model calculations give a good agreement with the experimental work, the EMPIRE maxima are slightly shifted to higher energy.

4.1.3 $^{nat}Sb(p, xn)^{123m}Te$ reaction

The radionuclide ^{123}Te has two isomeric states: the ground state with very long half-life ($T_{1/2} > 9.2 \times 10^{16}$ y) and an isomeric state with shorter half-life ($T_{1/2}$ = 119.2 d, level energy E_γ = 247.5 keV). The nuclei in the ground state are considered as stable due to the very long half-life. The ^{123}Te radionuclide can be produced only through the $^{123}Sb(p, n)$ reaction. The decay of the isomeric state is followed by one intense gamma line (E_γ = 159 keV) which interferes with the same energy gamma radiation emitted in the decay of ^{117m}Sn ($T_{1/2}$ =13.76 d). Although the $^{121}Sb(p, \alpha n)$ reaction has an energy threshold of about 2.5 MeV, the practical threshold is above 10 MeV due to the Coulomb barrier. Therefore in the present energy range this interference occurred only in the first two foils. The area of the measured photo peak at the energy of 159 keV was cumulative. Since the ^{123m}Te has a relatively long half-life as compared to that of ^{117m}Sn, about 50 days cooling time was applied to eliminate the contributions of the interfering radionuclide to the measured peak area.

The experimental data are presented in Figure 3 together with the EMPIRE 3.1 and TALYS 1.4 codes calculations and literature data.

The excitation function has a maximum at about 10 MeV with a cross section about 100 mb. The present experimental data show a good agreement with Takács et al. [4], while Singh et al. [5] have the same trend but with slightly higher values. The data obtained by TALYS-1.4 code are in good agreement with the experimental data, the EMPIRE-3.1 code also gives good agreement but with slightly higher values.

5 Yield calculation

The activation yields of $^{121m,g}Te$ and ^{123m}Te isotopes were calculated and are presented as a function of proton energy in Figure 4.

The three isotopes can be produced with acceptable activity at the present investigated energy range. So there production can be achieved at low energy cyclotrons but more suitable are medium energy cyclotrons. All of these

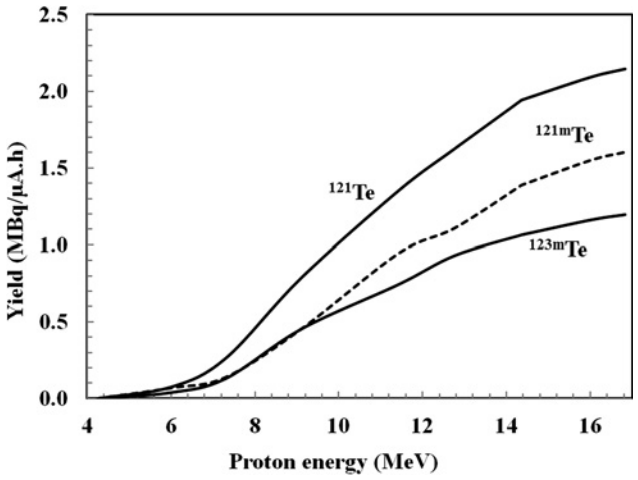

Fig. 4: Calculated integral yields of ^{121m,g}Te and ^{123m}Te as a function of proton energy.

isotopes have a relatively long half-life, and almost the same production threshold energy, so it is recommended to use enriched ^{121}Sb targets for their production. ^{121m,g}Te. If we use a natural target after appropriate cooling time ^{121m,g}Te decay to stable isotope ^{121}Sb and ^{123m}Te decays to the very long half-life ^{123g}Te. These tellurium isotopes are also formed in the production of the medical isotope ^{123}I.

6 Conclusion

The present work introduces a new experimental data set for the formation of the tellurium isotopes ^{121m,g}Te and ^{123m}Te between the previously measured data points which validate the form of the fitted excitation functions. The data were validated using the nuclear model calculations. A satisfactory agreement was achieved between the present results and the available literature data as well as the theoretical calculations.

Acknowledgement: The authors are greatly indebted to cyclotron crew of ATOMKI Debrecen, Hungary, for their help in irradiation of samples.

References

1. Qaim, S. M.: Nuclear data relevant to cyclotron produced short-lived medical radioisotopes. Radiochim. Acta **30**, 147(1982).
2. Qaim, S. M.: Nuclear data relevant to the production and application of diagnostic radionuclides. Radiochim. Acta **89**, 223 (2001).
3. Tárkányi, F., Király, B., Ditrói, F., Takács, S., Csikai, J., Hermanne, A., Uddin, M. S., Hagiwara, M., Baba, M., Ido, T., Shubin, Yu. N., Kovalev, S. F.: Activation cross sections on cadmium: proton induced nuclear reactions up to 80 MeV. Nucl. Instrum. Methods B **245**, 379 (2006).
4. Takács, S., Takács, M. P., Hermanne, A., Tárkányi, F., Adam Rebeles, R. : Cross sections of proton induced reactions on ^{nat}Sb. Nucl. Instrum. Methods B **297**, 44 (2013).
5. Singh, B. P., Sharma, M., Musthafa, M. M., Bhardwaj, H. D., Prasad, R.: A study of pre-equilibrium emission in some proton and alpha-induced reactions. Nucl. Instrum. Methods A **562**, 717 (2006).
6. Herman, M., Capote, R., Carlson, B. V., Obložinský, P., Sin, M., Trkov, A. Wienke, H., Zerkin, V., EMPIRE: nuclear reaction model code system for data evaluation. Nuclear Data Sheets **108**, 2655 (2007).
7. Herman, M., Capote, R., Sin, M., Trkov, A., Carlson, B. V., Obložinský, P., Mattoon, C. M., Wienke, H., Hoblit, S., Cho, Young-Sik, Plujko, V., Zerkin, V.: EMPIRE-3.1 Rivoli: modular system for nuclear reaction calculations and nuclear data evaluation (2012).
8. Koning, A. J., Hilaire, S., Duijvestijn, M. C.: TALYS-1.0, Proceedings of the International Conference on Nuclear Data for Science and Technology, 22–27 April, Nice, France (Bersillon, O., Gunsing, F., Bauge, E., Jacqmin, R., Leray, S., eds.) EDP Sciences (2008), pp. 211–214.
9. Hassan, H. E., Qaim, S. M., Shubin, Yu.,Azzam, A., Morsy, M., Coenen, H. H. : Experimental studies and nuclear model calculations on proton-induced reactions on ^{nat}Se, ^{76}Se and ^{77}Se with particular reference to the production of the medically interesting radionuclides ^{76}Br and ^{77}Br. Appl. Radiat. Isot. **60**, 899 (2004).
10. Hassan, K. F., Qaim, S. M., Saleh, Z. A., Coenen, H. H.: Alpha-particle induced reactions on ^{nat}Sb and ^{121}Sb with particular reference to the production of the medically interesting radionuclide ^{124}I. Appl. Radiat. Isot. **64**, 101 (2006).
11. Al-Abyad, M., Comsan, M. N. H., Qaim, S. M.: Excitation functions of proton-induced reactions on ^{nat}Fe and enriched ^{57}Fe with particular reference to the production of ^{57}Co. Appl. Radiat. Isot. **67**, 122 (2009).
12. Qaim, S. M., Stöcklin, G., Weinreich, R.: Excitation functions for the formation of neutron deficient isotopes of bromine and krypton via high-energy deuteron induced reactions on bromine: Production of ^{77}Br, ^{76}Br and ^{79}Kr. Int. J. Appl. Radiat. Isot. **28**, 947 (1977).
13. Ziegler, J. F., Ziegler, M. D., Biersack, J. P.: SRIM 2010 Code, Available from www.srim.org.
14. Tárkányi, F., Takács, S., Gul, K., Hermanne, A., Mustafa, M. G., Nortier, M., Obložinský, P., Qaim, S. M., Scholten, B., Shubin, Yu. N., Zhuang, Y.: "Beam monitor reactions": Charged Particle Cross-Section Database for Medical Radioisotope Production. TECDOC-1211, IAEA, Vienna (2001), pp. 49–152.
15. Kopecky, P.: Proton beam monitoring via the $Cu(p,x)^{58}Co$, $^{63}Cu(p,2n)^{62}Zn$ and $^{65}Cu(p,n)^{65}Zn$ reactions in copper. Int. J. Appl. Radiat. Isot. **36**, 657 (1985).
16. Piel, H., Qaim, S. M., Stöcklin, G.: Excitation functions of (p,xn)-reactions on ^{nat}Ni and highly enriched ^{62}Ni: possibility of production of medically important radioisotope ^{62}Cu at a small cyclotron. Radiochim. Acta **57**, 1 (1992).

17. Firestone, R. B.: Table of Isotopes. John Wiley and Sons, Inc., New York, USA (1998).
18. NUDAT-2.6 Database, http://www.nndc.bnl.gov/hbin/nudat.
19. Guide to Expression of Uncertainty in Measurements, ISO Geneva (1993), ISBN 92-10188-9.
20. Pritychenko, B., Sonzogni, A.: Q-value calculator, NNDC, Brookhaven National Laboratory, USA (2011). http://www.nndc.bnl.gov/qcalc.
21. EXFOR (2015). Nuclear reaction data, EXFOR is accessed on line at http://www.nndc.bnl.gov/exfor/exfor.htm.